

John K. Douglass · N. J. Strausfeld

Optic flow representation in the optic lobes of Diptera: modeling innervation matrices onto collators and their evolutionary implications

Accepted: 18 June 2000 / Published online: 26 August 2000
© Springer-Verlag 2000

Abstract A network model of optic flow processing, based on physiological and anatomical features of motion-processing neurons, is used to investigate the role of small-field motion detectors emulating T5 cells in producing optic flow selective properties in wide-field collator neurons. The imposition of different connectivities can mimic variations observed in comparative studies of lobula plate architecture across the Diptera. The results identify two features that are crucial for optic flow selectivity: the broadness of the spatial patterns of synaptic connections from motion detectors to collators, and the relative contributions of excitatory and inhibitory synaptic outputs. If these two aspects of the innervation matrix are balanced appropriately, the network's sensitivity to perturbations in physiological properties of the small-field motion detectors is dramatically reduced, suggesting that sensory systems can evolve robust mechanisms that do not rely upon precise control of network parameters. These results also suggest that alternative lobula plate architectures observed in insects are consistent in allowing optic flow selective properties in wide-field neurons. The implications for the evolution of optic flow selective neurons are discussed.

Key words Optic flow · Visual processing · Lobula plate · Computational maps · Evolution

Abbreviations *COM* center of motion · *SFMD* small-field motion detector

Introduction

Spatially mapped neural architectures are widely acknowledged to serve crucial roles in sensory infor-

mation processing (Knudsen et al. 1987). Classical examples include lateral inhibitory networks (Ratliff and Hartline 1974), orientation columns in mammalian visual cortex (Mountcastle 1957), and delay lines for analyses of phase differences in auditory and electrosensory systems (Carr 1986). Detailed neuroanatomical and physiological studies of how receptors map onto dendritic trees involved in processing mechanosensory inputs have provided new insights into the representation and computation of directional information in arthropods (e.g., Lockery and Kristan 1990; Jacobs and Theunissen 1996; Lewis and Kristan 1998). In Diptera, visual pathways serving directional motion-processing offer additional opportunities for understanding the functional significance of mapped neuropils. This is not only because these display great precision from one synaptic layer to the next (Strausfeld 1989), but also because phylogenetic differences in such maps relate to taxonomic differences in visually guided flight behaviors (Buschbeck and Strausfeld 1997).

In Diptera, as explained in a previous account (Douglass and Strausfeld 2000b), retinotopic arrays of T5 neurons are sensitive to motion direction (Douglass and Strausfeld 1995, 1996) and map their outputs onto the dendrites of wide-field collator neurons in the lobula plate. Neuroanatomical studies of calliphorid and muscid flies indicate that there are four T5 neurons per retinotopic column (Strausfeld and Lee 1991), and that individual T5 cell endings in the lobula plate are constrained to one of four functional levels that are activated by a specific direction and orientation of motion across the retina (Buchner and Buchner 1984). Thus, T5 cells carry information about directional motion to these specific functional levels, where wide-field collator neurons are activated by optic flow fields induced by rotations and translations about specific body axes (Hausen 1984; Krapp et al. 1998).

At first sight, the organized segregation of T5 terminals to motion and direction-sensitive strata suggests that this architectural arrangement reflects optimized connections for a flow-field processing system. A neuron

J. K. Douglass (✉) · N. J. Strausfeld
Arizona Research Laboratories Division of Neurobiology,
611 Gould-Simpson Bldg., University of Arizona,
Tucson, AZ 85721, USA
e-mail: jkd@neurobio.arizona.edu
Tel.: +1-520-621-9668; Fax: +1-520-621-8282

that responds exclusively to progressive motion would have its dendrites in a horizontal motion stratum, as is indeed the case in *Calliphora* and *Musca*. A neuron responding to composite horizontal and vertical flow fields, each separated at different regions on the retina, would have its dendrites in the two appropriate directional strata and at the corresponding retinotopic locations in the mosaic. This prediction is supported by the morphologies of certain “vertical” (VS) motion-sensitive neurons that have dendrites staggered at two levels of the neuropil (Hengstenberg 1982; Strausfeld and Bass-emir 1985; Krapp et al. 1998). If this architecture is especially important for visual flow processing, however, one would expect it to be conserved among visually active Dipterans.

Whereas comparative studies demonstrate that the T5 cells and a cohort of more peripheral neurons implicated in motion processing are ubiquitous to a variety of brachyceran and nematoceran Diptera (Buschbeck and Strausfeld 1996), lobula plate stratification and tangential neuron morphologies show great taxonomic diversity (Buschbeck and Strausfeld 1997). Tabanids (horse flies), for example, are highly maneuverable predators adept at avoiding defensive actions of their targets; the tabanid lobula plate is multistratified, containing many more horizontally oriented tangential neurons than in other groups. Many species of syrphids (hover flies) employ stationary as well as laterally directed hovering flight; their lobula plates are equipped with many more vertical tangential cells than in calliphorids or muscids. The long-bodied asilids (robber flies) make ballistic interceptions of their prey; their lobula plates entirely lack vertical tangential cells and are equipped with many small- and wide-field horizontal tangential cells. Despite such variations, each taxon presumably exploits information provided by optic flow. Clearly, the organization of optic flow processing neurons in the lobula plate need not conform to the calliphorid plan.

Computational properties of mapped neuropils are shaped by physiological as well as architectural features. Douglass and Strausfeld (2000b) demonstrated the sensitivity of an optic flow processing network based on T5-like motion detectors to physiological tuning properties of these small-field elements, and discussed the issue of whether the broadness of the small-field directional tuning can be optimized for optic flow processing. Although narrow tuning to sensory parameters is clearly useful in specialized contexts (Suga and Kanwal 1995), theoretical analyses have demonstrated remarkably efficient information transmission in broadly tuned, or “coarse-coded” networks (Heiligenberg 1987; Theunissen and Miller 1991). Though some workers have suggested that sensory tuning characteristics tend to be sharpened at successive processing levels (Levick et al. 1969; Glantz 1994), others argue that information transmission is more efficient and less subject to noise when the characteristics at successive levels are closely matched (Bialek and Owen 1990; Laughlin 1996).

Our model of optic flow processing (Douglass and Strausfeld 2000b) provides an opportunity to examine these issues as they apply to retinotopically organized directional information processing in the insect visual system. In the present account, we used an expanded version of the model to examine the effects of alternative wide-field innervation matrices (spatial patterns of synaptic connection strengths) on optic flow selectivity. The results show that although both small-field physiological properties and wide-field connection patterns can be optimized, the circuit’s properties may be so robust that significant departures from the “optimal” parameters are of little consequence for the performance of the network. Crucially, properties of successive processing levels do not have to be closely matched, suggesting that substantial variability in the evolutionary, developmental, or homeostatic processes that shape optic flow processing circuits is possible without endangering their most important computational properties. Thus, sensory systems across the animal kingdom may have evolved robust mechanisms that do not rely on precise network parameters.

Materials and methods

The same basic methods described in Douglass and Strausfeld (2000b) were employed here, with the addition of specific variations in properties of the innervation matrices. Briefly, a computational network with optic flow selective properties was designed based on specific anatomical and physiological features of motion processing pathways in calliphorid flies. The network (Fig. 1) was simulated by defining flow-field stimuli as arrays of local motion directions and speeds, computing analog (nonspiking) responses to these flow fields by four retinotopic arrays of small-receptive-field T5-like detectors (SFMDs), and pooling responses from selected SFMDs. The SFMD responses to be pooled were selected using innervation matrices, designed to generate selectivity for a particular type of optic flow when centered on the receptive field of a wide-field collator neuron. As in Douglass and Strausfeld (2000b), the external flow inputs always were defined to encompass the full receptive field of the collator.

The basic equations for responses of the local motion detectors (Douglass and Strausfeld 2000b) are functions of the local angular motion speed (S , degrees/s) and the direction (θ , degrees) of a moving edge, defined relative to the preferred direction of each SFMD:

$$R(\theta, S) = (b + 0.5 \cdot \cos(a \cdot \theta)) \cdot (k \cdot S \cdot e^{(1-k \cdot S)}), |\theta| < 180^\circ/a, \quad (1)$$

$$R(\theta, S) = (b - 0.5) \cdot (k \cdot S \cdot e^{(1-k \cdot S)}), |\theta| \geq 180^\circ/a,$$

where b specifies a constant offset from the zero response level and a determines the broadness of directional tuning. Each of the four SFMD arrays (Fig. 1A) was provided with one of four orthogonal preferred directions. Individual tests of the model employed one of four alternative small-field tuning functions with half bandwidths of either 180° [$R_A(\theta)$, $R_B(\theta)$; $a = 1$], or 90° [$R_C(\theta)$, $R_D(\theta)$; $a = 2$] as a function of motion direction, and either purely excitatory [$R_A(\theta)$, $R_C(\theta)$; $b = 0.5$], or balanced excitatory and inhibitory [$R_B(\theta)$, $R_D(\theta)$; $b = 0$] responses.

In the preceding account, the innervation matrices were composed of purely excitatory synaptic connections with equal synaptic weights, and the angular bandwidth of the retinotopic region represented by an individual matrix was fixed at 90° (Fig. 1Bi). In this account, instead of being limited to purely excitatory connections, matrices could be specified with both excitatory and inhibitory

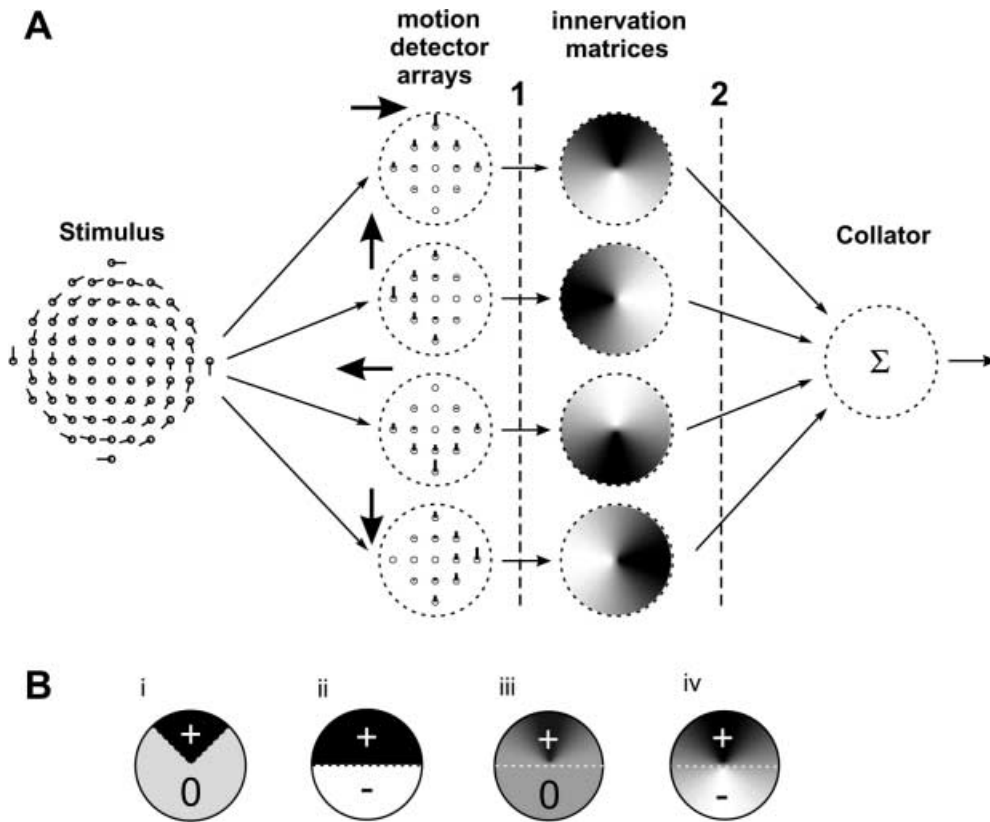


Fig. 1 **A** Overall architecture of the optic flow processing network. Optic flow stimuli, here a centered clockwise rotational flow, provide inputs to four superimposed arrays of small-field direction-sensitive motion detectors (SFMDs). The SFMD arrays have orthogonal preferred directions (*large arrows*), and response amplitudes (*vertical lines* at each SFMD location) are a function of local motion direction and speed (see Eq. 1). Gradient-type innervation matrices (spatial patterns of synaptic connection strengths), in this example designed to promote selectivity for clockwise flow, specify graded patterns of SFMD synaptic output strengths for linear summation by a wide-field collator neuron. The *darkest shading* represents strong excitatory synaptic connections; *lightest areas* represent strong inhibitory connections (see **B**). For simplicity, only 13 SFMDs are illustrated per array. Actual model computations used either 73 or 701 SFMDs per array (see Materials and methods). *Dotted vertical lines* (1 and 2) indicate processing levels that correspond to spatial activity patterns illustrated in Figs. 6 and 7. **B** Examples of alternative innervation matrices from SFMDs to a wide-field collator: **i** uniform matrix, 90° bandwidth with purely excitatory (+) connections (Eq. 2, matrix offset $s=0.5$); **ii** uniform matrix, 180° bandwidth with both excitatory and inhibitory (-) connections (Eq. 2, $s=0$); **iii** gradient matrix, 180° half bandwidth with purely excitatory connections (Eq. 3, $s=0.5$); **iv** balanced excitatory and inhibitory connections (Eq. 3, $s=0$)

synaptic connections (Fig. 1Bii,iv), the relative strengths of which were controlled by an offset in the equation for the innervation matrix (see below). This feature is consistent with the presence of both GABAergic (Strausfeld et al. 1995; Brotz and Borst 1996) and cholinergic inputs to wide-field lobula plate tangential neurons in the fly visual system (Brotz and Borst 1996). The angular bandwidths of innervation matrices were also varied, in order to investigate the consequences of narrow versus coarse spatial tuning of the retinotopic maps. Third, the innervation matrices were defined with either *uniform* distributions of synaptic weights (Fig. 1Bi,ii, as in Douglass and Strausfeld 2000b), or cosine-shaped synaptic weight *gradients* (Fig. 1Biii,iv). Matrix bandwidths and

half bandwidths were defined in terms of the angular extent of synaptic connections within the circular receptive field of a collator. Thus, the bandwidth of a uniform matrix is the range of angles within which excitatory synaptic connections were specified, and the half bandwidth of a gradient matrix is the angular width of the region in which excitatory synaptic strengths were $\geq 50\%$ of the maximum level.

Equations 2 and 3 (below) specify local synaptic strengths, w , for uniform- and gradient-type innervation matrices. The value of w depends on a constant offset s from zero, and on the angular bandwidth (bw) of a uniform matrix, or the half bandwidth (hbw) of a gradient matrix. This nomenclature for the broadness of uniform and gradient matrices, respectively, was used because the model outputs are very similar when the uniform matrix bandwidth and the gradient matrix half bandwidth are set to equal values (see Results).

Uniform innervation matrix

$$\begin{aligned} w &= s + 0.5, |\theta| \leq bw/2 \\ w &= s - 0.5, |\theta| > bw/2 \end{aligned} \quad (2)$$

Gradient innervation matrix

$$\begin{aligned} w &= s + 0.5 \cdot \cos(a \cdot \theta), |\theta| \leq hbw \\ w &= s - 0.5, |\theta| > hbw \end{aligned} \quad (3)$$

For a given collator neuron, the difference between maximal and minimal synaptic weights was kept constant at 1, and the matrix offset s could be varied between -0.5 and 0.5 . Setting $s=0.5$, for example, yielded purely “excitatory” synaptic weights from 0 to 1, whereas $s=0$ provided excitatory and inhibitory weights ranging in amplitude between -0.5 and $+0.5$. Absolute values of s greater than 0.5 were not tested, because they merely would have reduced the relative difference between minimum and maximum synaptic weights. In Eq. 3, the value of parameter a sets the half bandwidth of the innervation matrix: $hbw = 180^\circ/a$.

The model was written using Turbo Pascal (Borland International), and the figures were produced using Origin 5.0 (Microcal, Northampton, Mass.) and CorelDraw 6.0 and 8.0 (Corel, Ottawa, Ontario).

Results

As shown in the preceding account (Douglass and Strausfeld 2000b), the model shows robust selectivity to the position and type of optic flow. This is provided by using a small-field tuning function with broad directional tuning and both excitatory and inhibitory outputs (R_B), combined with a uniform, 90° bandwidth innervation matrix with unit synaptic weights (Eq. 2, $s=0.5$). Flow type selectivity is controlled by the angular positions of the innervation matrices within the retinotopic map, and can be adjusted to produce maximal responses to any flow type along a circular scale that includes pure clockwise rotation, pure expansion, counterclockwise rotation and contraction. Selectivity for flow type and position, however, is acutely sensitive to small-field tuning characteristics. Among the four alternative small-field functions R_A – R_D , strong flow type selectivity was obtained only with R_B . The actual characteristics of the small-field tuning functions and the innervation matrices of optic flow processing circuits in insects are poorly understood. Thus, the usefulness of this network as a model of neural circuitry rests on two major questions: (1) how sensitive are the R_B -based implementations to properties of the innervation matrix?, and (2) can alternatives to the original innervation matrix be identified which reduce the network's sensitivity to the small-field properties?

Large changes in map bandwidth and type have little effect on selectivity for flow type or position

Figure 2 illustrates the position and type selectivity of model implementations in which the positions of the innervation matrices were chosen to promote sensitivity to clockwise rotational flow (see Fig. 1A). The individual graphs compare responses to the preferred and anti-preferred optic flow types (clockwise and counterclockwise flow), orthogonal flow types (expansion and contraction), and unidirectional flow. The 12 graphs are arranged in three rows that illustrate the effects of innervation matrix half bandwidth (90°; 180°; 270°) on collator responses, and four columns that correspond to the four small-field motion detector tuning functions R_A – R_D , respectively. A 90° uniform innervation matrix with offset 0.5 (see Fig. 1Bi) was used in the original implementation of this model (Douglass and Strausfeld 2000b); all data in Fig. 2 were obtained using gradient innervation matrices, again with a matrix offset of 0.5 (e.g., Fig. 1Biii).

The effects of innervation matrix bandwidth on position and type selectivity (Fig. 2) are moderate changes in response amplitudes, regardless of the small-field

tuning function. Small-field tuning function R_B provides excitatory, position-sensitive responses to clockwise rotation, symmetrical inhibitory responses to counterclockwise flow, and virtually no response to expanding, contracting, or unidirectional flow. Thus, R_B produces the greatest selectivity for flow type and position and these properties are robust to changes in matrix bandwidth. On the other hand, since the poorer selectivities obtained with the other three small field functions are also relatively stable, changes to the bandwidth of the innervation matrix alone cannot reduce the network's sensitivity to its small-field tuning properties. The same tests shown in Fig. 2 for gradient matrices were also performed using the equivalent uniform matrices (bandwidths 90°, 180°, and 270°). The results were remarkably consistent with those shown here, with only small quantitative differences that do not alter the above conclusions. (For uniform matrix results that correspond to Figure 2A–D see Douglass and Strausfeld 2000b, Fig. 6E–H.)

Because of the robust flow selectivity associated with R_B , this small-field tuning function was used to further examine the sensitivity of the optic flow-processing network to innervation matrix broadness. Figure 3 shows responses of a collator to centered, preferred-type optic flow as a function of innervation matrix bandwidth for both uniform- and gradient-type matrices (note that the gradient data at 90°, 180°, and 270° correspond to position 0 of the continuous curves in Figure 2B, F, J). With both types of matrix, maximal responses were produced at intermediate bandwidths. This result is not surprising, because very narrow matrices carry few synaptic connections, whereas very broad matrices lack spatially specific information. The response maximum for uniform matrices, however, is 180°, while that for gradient matrices is 150° and only 82% as high. Another important difference is that gradient maps produce significant responses at half bandwidths as high as 360°.

What mechanisms are responsible for these differences between matrix types? Because the total synaptic weights to the collator neuron are nearly identical for a given uniform matrix bandwidth and gradient matrix half bandwidth, the differences must arise from interactions between the shapes of the innervation matrices and the spatial distributions of their small-field motion detector inputs. As defined in Eqs. 2 and 3, gradient maps are inherently broader, so the optimum map broadness occurs at a lower half bandwidth than for uniform maps. Meanwhile, the maximum response amplitude from gradient maps is reduced because less than 100% of the excitatory activity from small-field motion detectors is transferred, and because inhibitory activity is included which uniform maps only recruit at bandwidths greater than 180°. At 360°, the responses from uniform maps are equivalent to unspecialized, one-to-one mappings (Douglass and Strausfeld 2000b), for which the activities sum to zero in this case because the excitatory and inhibitory activities of the small-field detectors are symmetrical. With 360° half bandwidth

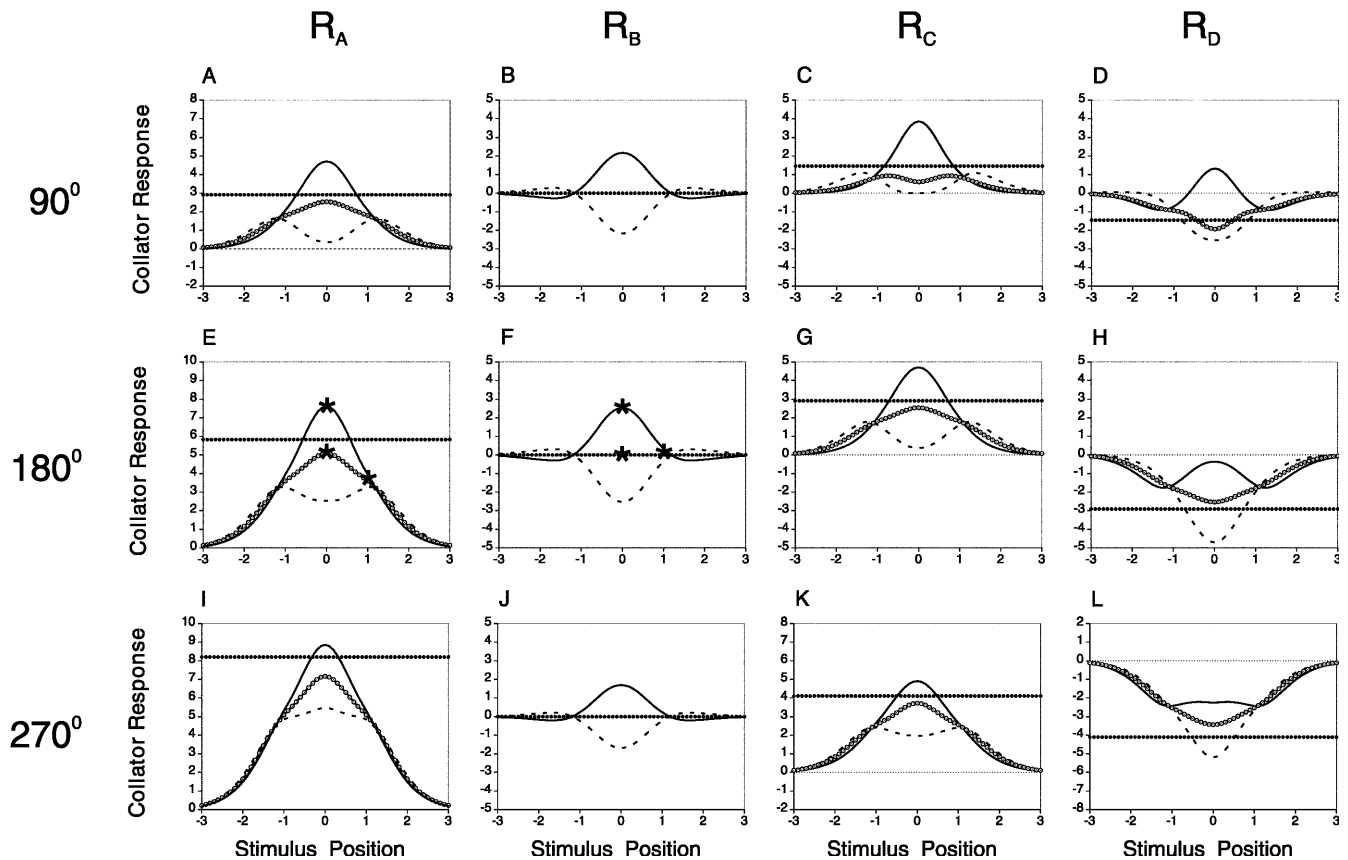


Fig. 2 Comparison of position and type selectivity as a function of small-field motion detector tuning (*columns*) and innervation matrix bandwidth (*rows*), with the matrix offset (Eq. 3) set at 0.5. All data are from networks with gradient innervation matrices designed to produce maximal responses to pure clockwise rotation that is centered in the middle of the collator receptive field (position 0; see Materials and methods and Fig. 1). Column labels refer to the respective small-field tuning functions R_A – R_D (Materials and methods, Eq. 1). Row labels indicate innervation matrix half bandwidths of 90° , 180° , and 270° . *Abscissa*, flow field position in units of receptive field radii. Each graph shows responses to clockwise rotation (*solid lines*), counterclockwise rotation (*dotted*), pure expansion or pure contraction (*open circles*), and unidirectional flow (*closed circles*). With small-field tuning function R_B , responses to expansion, contraction and unidirectional flow were always zero. *Asterisks* correspond to spatial activity patterns illustrated in Fig. 6 (see text for details)

gradient maps, however, the spatial distribution of synaptic strengths remains slightly nonuniform, thus favoring the transmission of excitatory responses.

Combined adjustments to innervation map bandwidth and offset optimize selectivity for flow position and type

Up to this point, tests of alternative innervation matrix shapes and bandwidths have confirmed the previous result (Douglass and Strausfeld 2000b) that the small-field directional tuning function R_B is the best suited for generating optic flow selectivity. Also, alternative matrix shapes have failed to reduce the sensitivity of the net-

work to perturbations in small-field properties. However, the optic flow selectivity data from small-field tuning functions R_A , R_C and R_D (Fig. 2), suggest two additional strategies. Two defining characteristics of R_B -based implementations, both of which are crucial for optic flow selectivity but are missing from the other data in Fig. 2, are the symmetry between responses to pre-

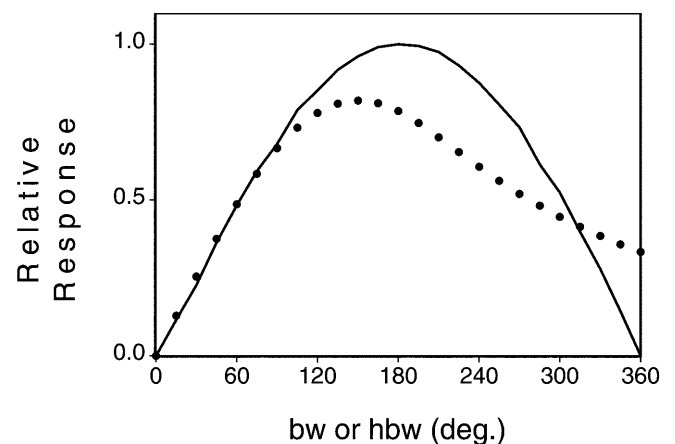


Fig. 3 Effect of innervation matrix spatial properties (*bw*, uniform matrix bandwidth; *hbw*, gradient matrix half bandwidth) on network response to centered clockwise rotation, using small-field tuning function R_B with uniform (*continuous curve*) or gradient (*dotted curve*) innervation matrices. Responses are normalized to the uniform matrix maximum at 180° . Computed using 701 SFMDs per array

ferred and antipreferred flows, and the zero responses to unidirectional and orthogonal flows. Data from R_A , R_C and R_D show a clear trend toward these characteristics as the map bandwidth is reduced. This suggests that further reduction in map bandwidth will cause the non- R_B -based networks to behave more like an R_B -based implementation. So far, however, only innervation matrices with purely excitatory "synapses" ($s = 0.5$ in Eq. 2) have been investigated. Thus, a second and more powerful strategy is to include negative (inhibitory) weights in innervation matrices by varying the offset s between -0.5 and 0.499 . If the relative strengths of excitatory and inhibitory outputs can be appropriately balanced, this could produce the desired symmetry in responses of non- R_B -based implementations to preferred and antipreferred inputs.

These two possibilities were examined by finding the matrix offset which minimizes the sum of collator responses to preferred and antipreferred flows, thereby maximizing the symmetry between these responses (Fig. 4). Data for networks endowed with R_B have been omitted from this figure, because their collator responses are independent of the innervation matrix offset and the above sum is always zero. For functions R_A , R_C , and R_D , this sum falls to zero upon optimization of the offset. With the exception of R_B , the original offset of 0.5 is suited only for very narrow innervation matrices that are otherwise undesirable because they produce low response amplitudes. The optimized offsets differ for each of the other small-field tuning functions, but all converge to zero at a half bandwidth of 180° . As noted above for R_B , the collator response amplitude is a function of map bandwidth (Fig. 3). In R_A -, R_C -, and R_D -based networks with optimized innervation matrix offsets, collator response amplitudes vary in the same manner (data not shown). The response amplitudes for R_A and R_B are identical, and those obtained with the narrower small-field tuning of R_C and R_D are reduced, but only by a maximum of about 20%.

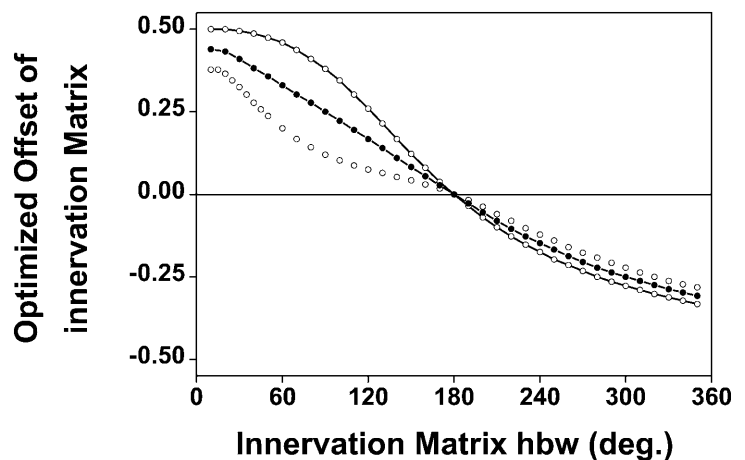
Figure 4 demonstrates that optimization of map offsets minimizes the absolute difference between responses to preferred and antipreferred flow types, but how does

this adjustment affect sensitivity to flow position, and responses to non-preferred flow types? Figure 5 illustrates position and type selectivity for the same model parameters used in Fig. 2, but now using the optimized innervation matrix offsets in Fig. 4. There has been a dramatic reduction in the sensitivity of responses to changes in both small-field tuning (Fig. 5, columns) and innervation matrix bandwidth (Fig. 5, rows). Nearly all response patterns now closely resemble that of small-field function R_B . With small-field function R_A , responses to the orthogonal flow types have essentially been eliminated, and the symmetry between responses to preferred and antipreferred flow types is position dependent in the same manner as for R_B . With the narrower small-field functions R_C and R_D , the response patterns are less symmetrical at the narrower (90°) map bandwidth, and attenuated with the broader (270°) map. Nevertheless, there is a remarkable convergence toward the R_B pattern. In conclusion, optimization of map offsets dramatically reduces the dependence of the optic flow-processing network on other basic properties of the wide-field innervation matrices and SFMDs. Although the small-field function R_B is clearly unique in its versatility and its insensitivity to map offsets, the effects of a broad range of alternative small-field functions are virtually indistinguishable from those of R_B if combined with an appropriately adjusted innervation matrix.

Mechanisms of selectivity for optic flow type and position

The interaction between wide-field retinotopic maps and the small-field physiological properties of individual motion detectors can be visualized by examining predicted spatial activity patterns within arrays of SFMDs and within the receptive field of a collator. Predicted spatial patterns of "presynaptic" activity produced by the small-field tuning functions (Fig. 1A, processing level 1) have been discussed previously (Douglass and Strausfeld 2000b). Figures 6 and 7 show examples of

Fig. 4 The relationship between gradient innervation matrix half bandwidth (*abscissa*) and the innervation matrix offset (*ordinate*) required to equalize the absolute values of the responses to preferred and antipreferred optic flow. Data are shown for the small-field tuning functions R_A (\bullet), R_C ($-\circ-$), and R_D (\circ), but not for function R_B , which produces equalized responses at all combinations of offset and half bandwidth. All four tuning functions produce a maximal collator response amplitude at 150°



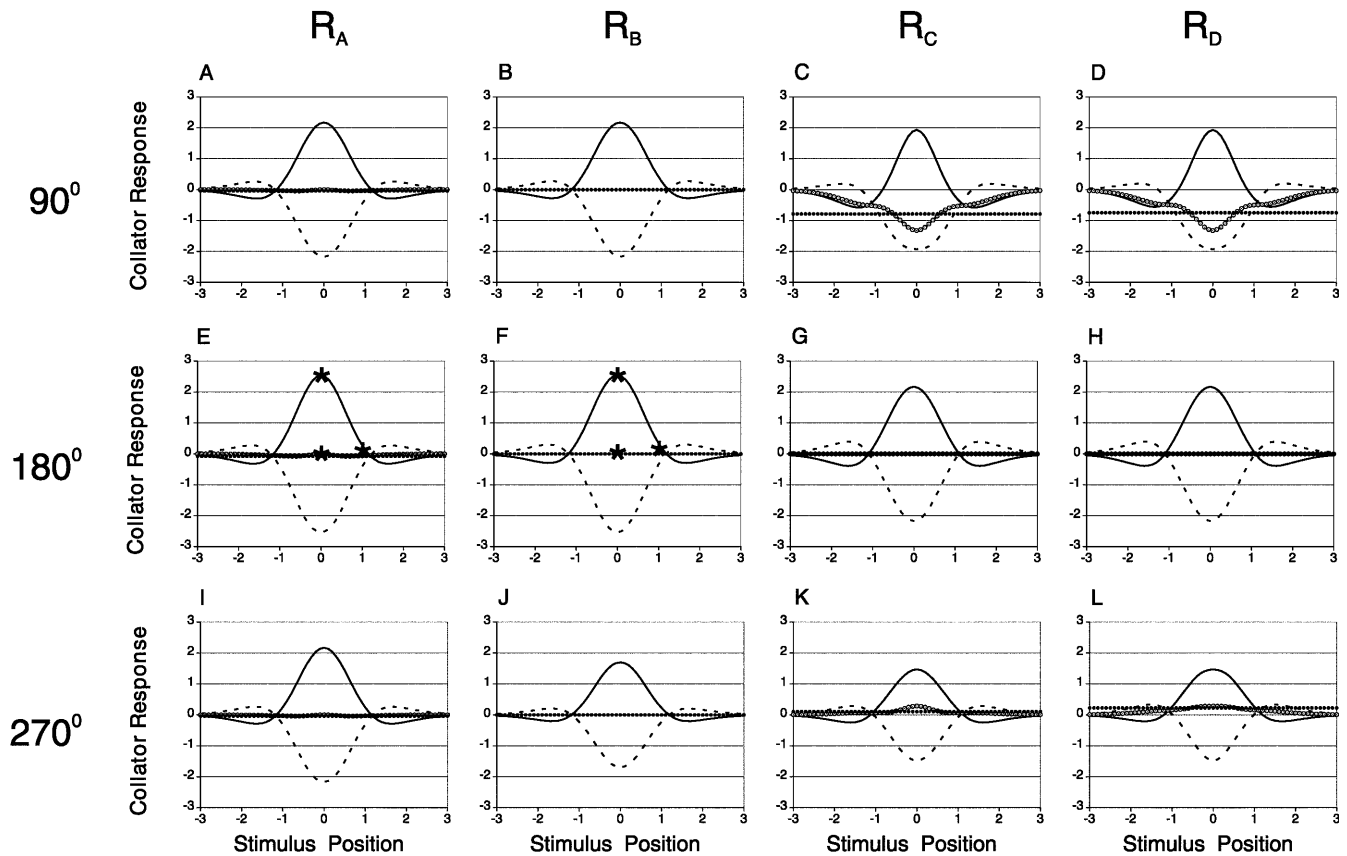


Fig. 5 Position and type selectivity as a function of SFMD tuning (columns) and innervation matrix bandwidth (rows). The sensitivity to small-field tuning (columns) and innervation matrix bandwidth (rows) has been minimized by using the optimized innervation matrix offsets in Fig. 4, or zero offsets for small-field tuning function R_B . The figure formatting and other network parameters are the same as in Fig. 2. Asterisks correspond to spatial activity patterns illustrated in Fig. 7 (see text for details)

“postsynaptic” activity patterns (Fig. 1A, level 2) in model implementations that combine small field tuning functions R_A or R_B with a 180° gradient innervation matrix designed to promote responses to centered, clockwise rotation. Responses to pure clockwise rotation and pure expansion are shown for centered flows (position 0) and for flows that are displaced by one receptive field radius from the collator receptive field center (position 1). In Fig. 6, the innervation matrix offset is $+0.5$, a value that has been shown to be poorly suited for optic flow selectivity with R_A (see Fig. 4). In Fig. 7, the 180° innervation matrix offset was 0, which is optimal for both R_A and R_B (Fig. 4). The data marked with asterisks in Fig. 2 show the spatially summed collator outputs from Fig. 6, and those marked in Fig. 5 correspond to Fig. 7.

When small-field tuning function R_A is combined with the $+0.5$ map offset (Fig. 6, left side), individual motion detector arrays produce only excitatory responses (color coded red), and all model synapses are also excitatory. Thus, although centered clockwise rotation produces excitatory responses, so do expansion

and both types of displaced flow (see Fig. 2E, asterisks). Response amplitudes approach zero (green) only at flow displacements so large that the local flow speeds exceed the speed response maxima of individual motion detectors (Douglass and Strausfeld 2000b). In contrast, individual small-field detectors tuned to R_B (Fig. 6, right side) can generate either excitatory or inhibitory responses. With centered rotation, the purely excitatory innervation matrices exclude most of the inhibitory activity, so the summed collator response is strongly excitatory. With expansion and displaced flows, however, the regions of excitatory and inhibitory small-field activity are shifted with respect to the innervation matrices just enough so as to sum to zero at the level of final collator outputs (Fig. 2F, asterisks).

As we have seen, a zero-offset innervation matrix reduces the network’s sensitivity to small-field tuning properties. Examination of spatial activity patterns (Fig. 7) illustrates the manner in which this effect could arise. Because the innervation matrices now incorporate both excitatory and inhibitory weights (see Materials and methods), local postsynaptic activity levels are altered in such a way that the summed spatial activity patterns for R_A (Fig. 7, bottom left plots) are indistinguishable from their R_B -based counterparts (Fig. 7, bottom right plots). Thus, to the extent that local summation of SFMD inputs is linear, the model predicts that insensitivity to small-field tuning can be established locally, and should not be affected by subsequent nonlinearities in collator dendritic integration.

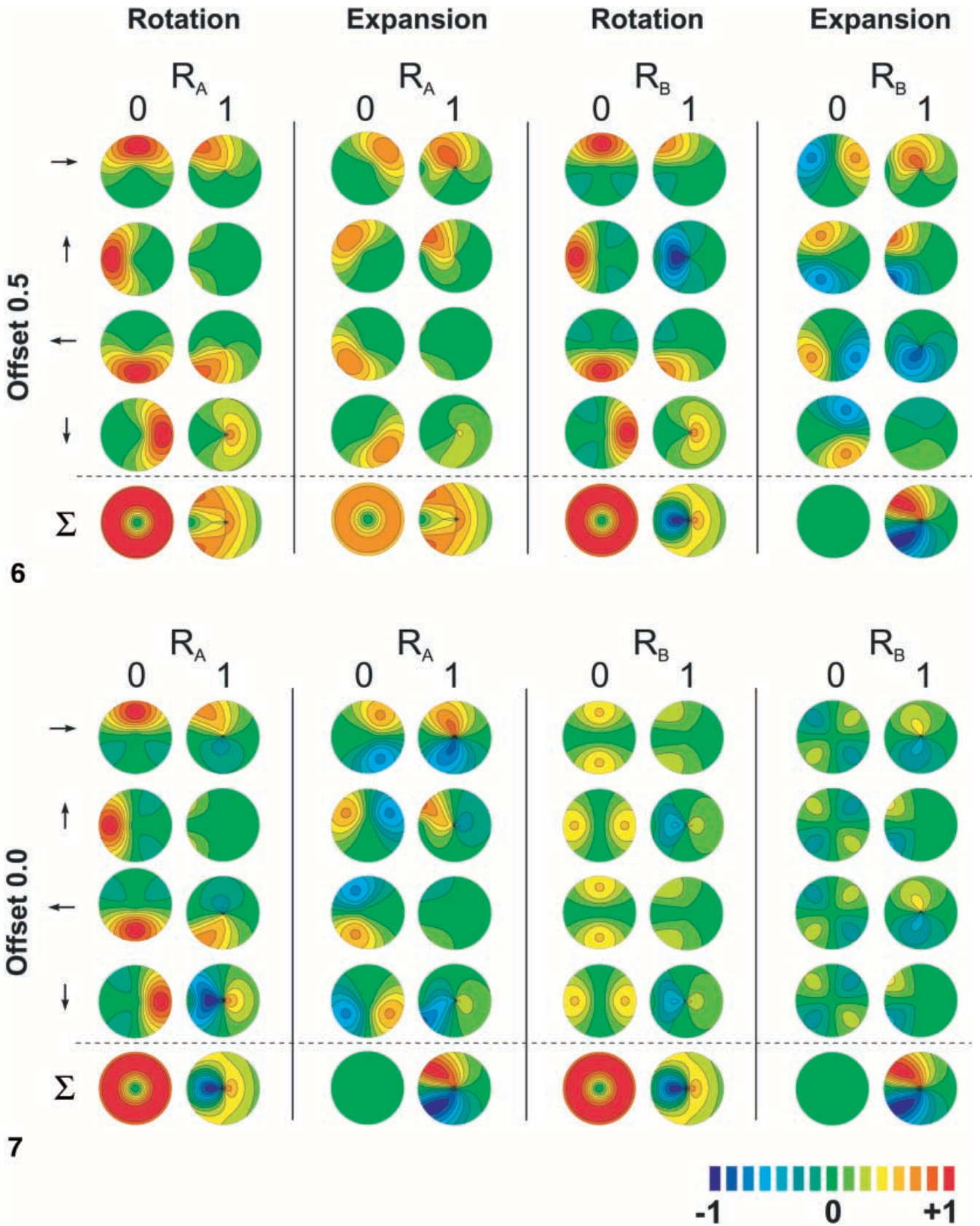




Fig. 6 Spatial patterns of flow type and position selectivity generated with purely excitatory, 180° half bandwidth innervation matrices having an offset of 0.5. The contour plots show predicted “postsynaptic” population responses of SFMDs, corresponding to level 2 in Fig. 1A. Responses are calculated for four arrays of SFMDs, each array having an orthogonal preferred direction indicated by the *arrows* at left. Responses to pure clockwise rotation and pure expansion are shown for two of the four alternative small-field directional tuning functions (R_A and R_B) during centered flow (*Position 0*) and flow positioned at the edge of the collator receptive field (*Position 1*). Note that directional tuning functions R_A and R_B share a 180° half bandwidth, but R_A is purely excitatory, whereas R_B is both excitatory and inhibitory. Contour colors depict response amplitudes ranging from strongly excitatory (*red*) to strongly inhibitory (*blue*). Summed (Σ) and individual array responses are plotted using the same color scale, which is normalized to the overall maximum and minimum summed response amplitudes

Fig. 7 Flow type and position selectivity, plotted as in Fig. 6, but generated using 180° half bandwidth innervation matrices with an offset of 0.0. With this innervation matrix offset, the sensitivity to small-field tuning properties is reduced. The summed responses of the R_A - and R_B - based networks are identical

Discussion

The results show that when the optic flow processing network is implemented by using purely excitatory innervation matrices the performance of the network is sensitive to physiological perturbations of small-field motion detectors that emulate T5 cells (see also Douglas and Strausfeld 2000b). The present investigation has shown that this frailty can be greatly reduced through the use of alternative innervation matrices. Two basic strategies were successful in this regard: (1) setting the half bandwidths of the innervation matrices at 180° and assigning equal areas to excitatory and inhibitory synapses, and (2) optimizing the innervation matrix offsets according to the small-field tuning properties and the innervation matrix bandwidth. Uniform and gradient matrices produced nearly identical outputs, suggesting that the precise shape of the innervation matrix is less important than its bandwidth or the balance between excitation and inhibition. Since there is evidence for both GABAergic and cholinergic inputs to lobula plate collators (Egelhaaf et al. 1990; Strausfeld et al. 1995; Brotz and Borst 1996), it is reasonable to suppose that T5 connections to these neurons can include both excitatory and inhibitory synapses. If so, then the model would predict that T5 directional tuning profiles can vary substantially without significantly affecting the optic flow selective properties of collator neurons.

Filtering of spatial information by summation of population-coded activity

This study has focused on mechanisms by which a collator can encode information about the optic flow type

and the radial distance of the center of motion (COM) from the center of the collator’s receptive field. Other information is present in the predicted patterns of spatial activity within the collator dendrites, but is lost during summation of the local activity levels. For example, when a flow field is displaced from the receptive field center, it generates distinctive regions of excitatory and inhibitory activity that clearly reveal the angular orientation of the COM with respect to the collator (see summed activities in Figs. 6 and 7, position 1). Though in principle this information could be extracted at this processing level by a neuron that is selective for the orientations of the excited and inhibited regions, changes in the COM angular orientation could be confounded with responses to non-preferred flow types (cf. summed responses to rotation and expansion, Figs. 6 and 7). Thus, the model suggests that the COM orientation would be more reliably discriminated by comparing, at a deeper level of the system, responses of several collators with partially overlapping receptive fields, each centered on a different part of the visual surround. If so, it would be expected that Diptera which exploit optic flow for precise visual control, as in hovering flight or avoidance flight, should have their retinotopic mosaic parceled by large numbers of relatively small tangential neurons. Indeed, this kind of arrangement is typical of the syrphids (hover flies), which are excellent at hovering, and tabanids (horseflies), which are specialized for predator avoidance (Buschbeck and Strausfeld 1997).

Optimizing a directional mosaic network for selectivity or robustness to change

Is there a unique set of parameters that maximizes the performance of this network? Using the small-field tuning function R_B , maximal response amplitudes were obtained at a half bandwidth of 150° for gradient innervation matrices, and 180° for uniform matrices (Fig. 3). For both types of matrix, however, 180° is the only bandwidth where optic flow selectivity was completely stable to changes in small-field tuning properties without requiring a synaptic offset adjustment (Fig. 4). Thus, optimizing the response amplitude does not necessarily optimize robustness to perturbations. Although other network parameters could be more precisely optimized, a striking feature of this network is that this precision is unnecessary. The patterns of selectivity for flow type and position are remarkably consistent across a wide range of model parameters, and response selectivity suffers little from significant changes in these parameters. For example, Fig. 3 shows that varying the half bandwidth of a gradient innervation matrix by $\pm 40^\circ$ from its 150° optimum, or a uniform matrix bandwidth by $\pm 45^\circ$ from the 180° optimum, reduces the response to centered, preferred-type flow by only 10%. Similarly, with innervation matrix offsets optimized as in Fig. 5, reducing the small-field tuning bandwidth by 50% (from R_A to R_C , or

R_B to R_D) reduces the collator responses by far less, particularly for innervation matrix half bandwidths between 90° and 180° . In conclusion, significant variability in the parameters of such a network will not seriously compromise the optic flow processing properties, whether the variability originates in physiological processes that affect small-field tuning properties, developmental processes that control innervation matrix formation, or evolutionary processes that lead to divergent lobula plate architectures.

Evolutionary and developmental flexibility without sacrificing performance

The robustness of optic flow selectivity in this model to variations in both small-field tuning properties and the properties of wide-field innervation matrices has important implications regarding the evolution and development of optic flow-processing networks. These implications may extend to similar networks that process spatially mapped temporal changes, including sensory modalities other than vision. Because changes in the parameters of this network have relatively minor consequences for computational properties, the establishment of connections between T5 cells and optic flow-selective collators may not be subject to the strict precision that characterizes more peripheral processing levels of arthropod visual systems (e.g., Snyder and Menzel 1975). The same robustness to variations may also have facilitated evolutionary diversity in neural architectures for visual motion processing, for which there is anatomical evidence both within the Diptera (Buschbeck and Strausfeld 1997) and across a wide range of other insect taxa (Strausfeld 1998; Douglass and Strausfeld 1999).

Model implications for neural architectures that process optic flow

Does this model require specific architectural features to be present in the lobula plate, and do the alternative innervation matrix configurations predict corresponding differences in lobula plate architecture? In the Introduction, we noted that the lobula plates of muscid, calliphorid and drosophilid flies are functionally subdivided into four distinct strata, each selective for visual motion in one of four orthogonal directions. Directional motion-sensitive T5 cells supplying wide-field collators generally restrict their lobula plate terminals to one of these four strata (Strausfeld 1989; Fischbach and Dittich 1989). However, are layered directional maps crucial to the organization of directional motion processing, and must the organization of collators conform to a stratified organization? Clearly this need not be the case, since numerous Diptera depart from the calliphorid type. The following illustrates four arrangements that correspond to known lobula plate architectures and are

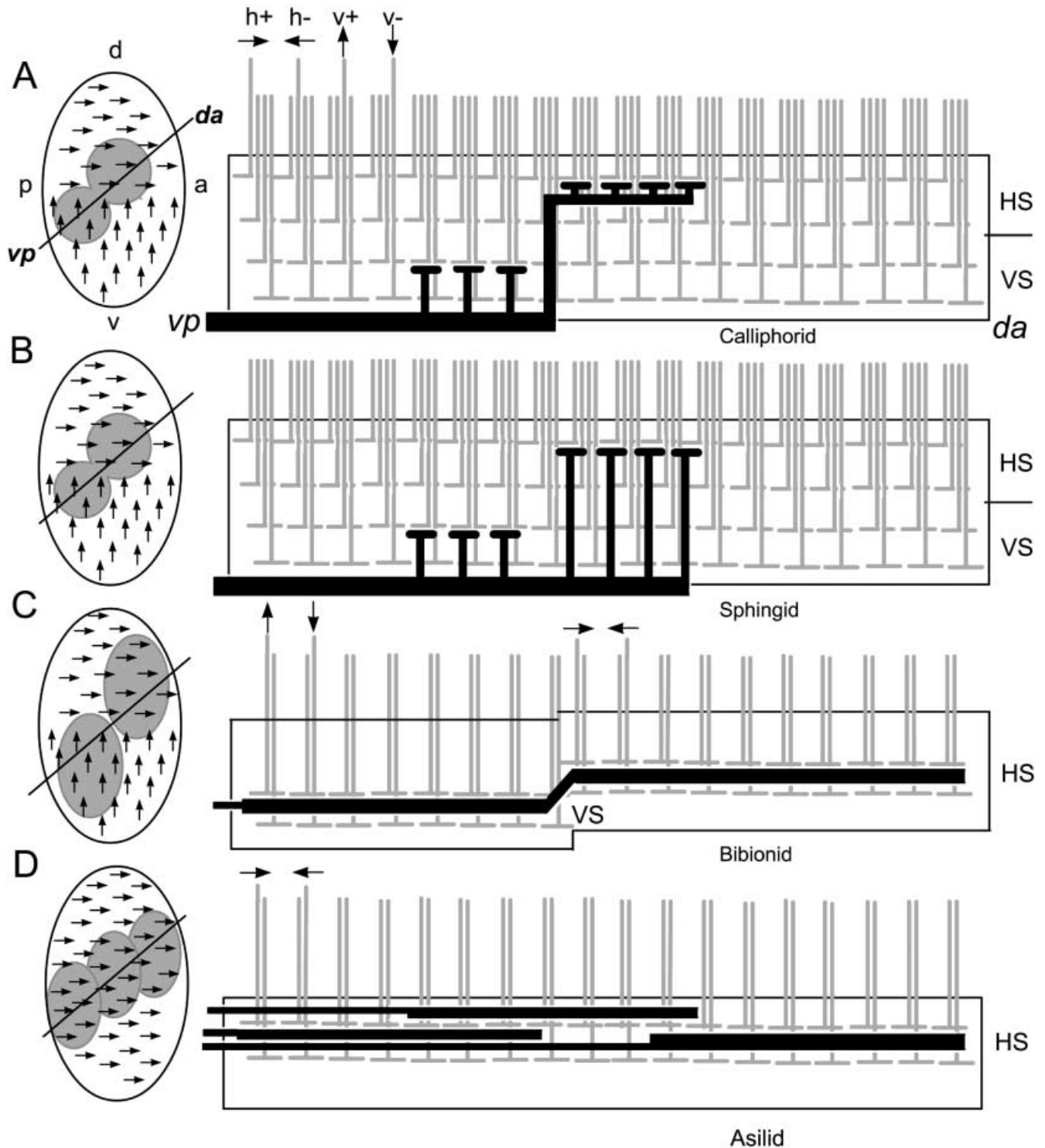
compatible with the alternative innervation matrices modeled here.

The first two architectures (Fig. 8A, B) restrict the terminals of individual T5 cells to one of the four direction-selective strata in the lobula plate, as suggested above. In the first architecture (Fig. 8A), the collator has a bistratified morphology with its trunk staggered at two different levels in the lobula plate, where it provides postsynaptic dendritic branches. This arrangement has been observed for the VS 1 neuron in the blowfly *Calliphora* (Hengstenberg 1982), which has its dorsal dendrites in the horizontal motion sensitive strata and ventral dendrites in vertical motion sensitive strata. The VS5–VS11 neurons also have many of their dorsal dendrites likewise disposed (Strausfeld and Bassemir 1985), and are sensitive to rotational stimuli (Krapp et al. 1998). These neurons are presynaptic to descending neurons that drive head roll (Milde and Strausfeld 1986). Krapp et al. (1998) suggest that horizontal directional preferences can also be found in VS dendrites that are restricted only to vertically sensitive strata (VS2, 3, 4 in *Calliphora*). These authors propose that this sensitivity to horizontal motion is achieved by small-field interneurons that link T5 terminals in the horizontal motion sensitive layer with VS dendrites situated in the vertical motion-sensitive layer. Thus far no evidence has been put forward to support this, whereas even VS cells with most dendrites restricted to one

Fig. 8A–D T5 organization is evolutionarily constrained across the Nematocera and Brachycera, as well as across the Lepidoptera, with taxon-specific differences relating only to the depth of penetration of T5 cells into the lobula plate and the number of T5 channels for each visual sampling point. The arrangements of collators vary across taxa, however (Buschbeck and Strausfeld 1997). In the figures at left, two directions of visual flow are shown across schematized eyes (*a* anterior, *p* posterior, *d* dorsal, *v* ventral, *vp* ventro-posterior, *da* dorso-anterior), and shaded areas represent receptive fields of collator neuron(s). The figures to the right show sections of the lobula plate, the orientation of which is shown by the oblique line across the schematic at left. The collators are diagrammed in profile against the T5 arrays, and T5 preferred directions are shown as *H+* horizontal progressive, *H-* regressive, *V+* upward vertical motion, and *V-* downward vertical motion. Trunks of collator cells can be positioned at various levels in lobula plate strata (**A**), as in cyclorrhaphan Diptera. Alternatively, local differences in dendritic stratification arise from unistratified trunks, as in Lepidoptera (**B**). In both, sensitivity to upward vertical and progressive horizontal motion on the retina will correspond to the location of dendrites within appropriate strata of the lobula plate. **C** A different solution to obtaining information about two directions of motion has been achieved in certain nematocerans, such as male bibionids, in which the retina and underlying neuropils are divided dorsoventrally. The lobula plate contains collators with vertical dendrites in its lower half, and horizontal dendrites in its upper half. This arrangement suggests that exclusively vertical motion-sensitive T5s supply the ventral part of the lobula plate, and exclusively horizontal motion-sensitive T5 cells supply the dorsal half. **D** Transformation of two of the four T5 arrays may have evolved in asilids (robber flies). Numerous HS-like cells, each with a small dendritic field, form planar ensembles across the lobula plate. There are no vertical cells. The lobula plate possesses only one layer of T5 endings, suggesting loss of sensitivity to vertical motion

stratum send occasional processes distally to the horizontal motion sensitive layer. This typifies a morphology, typical of sphingid moths and observed in *Drosophila* and other Diptera (Cajal and Sánchez 1915; Strausfeld 1970; Fischbach and Dittrich 1989), of collators equipped with a tangential trunk that is resident in a single stratum but which gives rise to dendritic

branches that can ascend into the appropriate horizontal motion sensitive strata (Fig. 8B). A third architecture (Fig. 8C) allows the collator itself to be unistratified while different areas of the planar unistratified lobula plate are tuned to different directional sensitivities. Morphological evidence for this arrangement is found in the lobula plates of certain nematocerans, like the bi-



bionids (March flies) (Buschbeck and Strausfeld 1997), in which upper and lower eye halves serve different functions and are likely to be sensitive to different flow directions (Zeil 1979), yet both halves supply a common lobula plate. Finally, lobula plate architectures may be specialized to provide only one directional sensitivity while retaining the evolutionarily conserved architecture of stratified ensembles of T5 endings (Fig. 8D). This arrangement has been suggested in robber flies (Asilidae) in which the lobula plate is unistratified and contains many horizontal-like collator neurons visited by the terminals of T5 cells (Buschbeck and Strausfeld 1997).

In summary, a variety of lobula plate architectures are compatible with robust optic flow selectivity in this model. Future research that investigates both physiological and anatomical properties of optic flow-sensitive neurons across taxa will reveal which of these architectures correspond most closely to actual circuits.

Acknowledgements The development of this model has benefited from discussions with Dr. Charles M. Higgins, Dr. Mandyam V. Srinivasan provided helpful comments on an early version of the manuscript. Grant sponsors: AFOSR 980803 (to JKD); NIH NCRN RO1 08688; ONR N00014-97-1-0970 (to NJS).

References

- Bialek W, Owen WG (1990) Temporal filtering in retinal bipolar cells, elements of an optimal computation. *Biophys J* 58: 1227–1233
- Brotz TM, Borst A (1996) Cholinergic and GABAergic receptors on fly tangential cells and their role in visual motion detection. *J Neurophysiol* 76: 1786–1799
- Buchner E, Buchner S (1984) Neuroanatomical mapping of visually induced neuron activity in insects by 3H-deoxyglucose. In: Ali MA (ed) *Photoreception and vision in invertebrates*. Plenum Press, New York, pp 623–634
- Buschbeck EK, Strausfeld NJ (1996) Visual motion detection circuits in flies: small-field retinotopic elements responding to motion are evolutionarily conserved across taxa. *J Neurosci* 16: 4563–4578
- Buschbeck EK, Strausfeld NJ (1997) The relevance of neural architecture to visual performance: phylogenetic conservation and variation in dipteran visual systems. *J Comp Neurol* 383: 282–304
- Cajal SR, Sánchez D (1915) Contribución al conocimiento de los centros nerviosos de los insectos. Parte I. Retina y centros opticos. *Trab Lab Invest Biol Univ Madrid* 13: 1–167
- Carr CE (1986) Time coding in electric fish and barn owls. *Brain Behav Evol* 28: 122–133
- Douglass JK, Strausfeld NJ (1995) Visual motion detection circuits in flies: peripheral motion computation by identified small-field retinotopic neurons. *J Neurosci* 15: 5596–5611
- Douglass JK, Strausfeld NJ (1996) Visual motion-detection circuits in flies: parallel direction- and non-direction-sensitive pathways between the medulla and lobula plate. *J Neurosci* 16: 4551–4562
- Douglass JK, Strausfeld NJ (1999) Evolutionary convergence of visual neuropils possibly involved in motion processing. *Soc Neurosci Abstr* 25: 905
- Douglass JK, Strausfeld NJ (2000a) Pathways in dipteran insects for early visual motion processing. In: Zanker JM, Zeil (eds) *Motion vision: Computational, neural and ecological constraints*. Springer, Berlin Heidelberg New York, 67–81
- Douglass JK, Strausfeld NJ (2000b) Optic flow representation in the optic lobes of Diptera: modeling the role of T5 directional tuning properties. *J Comp Physiol A* (in press) DOI 10.1007/s003590000131
- Egelhaaf M, Borst A, Pils B (1990) The role of GABA in detecting visual motion. *Brain Res* 509: 156–160
- Fischbach K-F, Dittrich APM (1989) The optic lobe of *Drosophila melanogaster*. I. A Golgi analysis of wild-type structure. *Cell Tissue Res* 258: 441–475
- Franceschini N (1975) Sampling of the visual environment by the compound eye of the fly: fundamentals and applications. In: Snyder AW, Menzel R(eds) *Photoreceptor optics*. Springer, Berlin Heidelberg New York, pp 98–125
- Glantz R (1994) Directional selectivity in a nonspiking interneuron of the crayfish optic lobe: evaluation of a linear model. *J Neurophysiol* 72: 180–193
- Hausen K (1984) The lobula complex of the fly: structure, function and significance in visual behavior. In: Ali MA (ed) *Photoreception and vision in invertebrates*. Plenum Press, New York, pp 523–599
- Heiligenberg W (1987) Central processing of sensory information in electric fish. *J Comp Physiol A* 161: 621–631
- Hengstenberg R (1982) Common visual response properties of giant vertical cells in the lobula plate of the blowfly *Calliphora erythrocephala*. *J Comp Physiol A* 149: 179–193
- Jacobs GA, Theunissen FE (1996) Functional organization of a neural map in the cricket cercal sensory system. *J Neurosci* 16: 769–784
- Knudsen EI, Lac S du, Esterly SD (1987) Computational maps in the brain. *Annu Rev Neurosci* 10: 41–65
- Krapp HG, Hengstenberg B, Hengstenberg R (1998) Dendritic structure and receptive-field organization of optic flow processing interneurons in the fly. *J Neurophysiol* 79: 1902–1917
- Laughlin SB (1996) Matched filtering by a photoreceptor membrane. *Vision Res* 36: 1529–1541
- Levick WR, Oyster CW, Takahashi E (1969) Rabbit lateral geniculate nucleus: sharpener of directional information. *Science* 165: 712–714
- Lewis JE, Kristan WB Jr (1998) Quantitative analysis of a directed behavior in the medicinal leech: implications for organizing motor output. *J Neurosci* 18: 1571–1582
- Lockery SR, Kristan Jr WB (1990) Distributed processing of sensory information in the leech. II. Identification of interneurons contributing to the local bending reflex. *J Neurosci* 10: 1816–1829
- Milde JJ, Strausfeld NJ (1986) Visuo-motor pathways in arthropods. *Naturwissenschaften* 73: 151–154
- Mountcastle VB (1957) Modality and topographic properties of single neurons in cat's somatic sensory cortex. *J Neurophysiol* 20: 408–434
- Ratliff F, Hartline HK (1974) *Studies of excitation and inhibition in the retina: a collection of papers from the laboratories of H. Keffer Hartline*. The Rockefeller University Press, New York
- Snyder AW, Menzel R (1975) *Photoreceptor optics*. Springer, Berlin Heidelberg New York
- Strausfeld NJ (1970) Golgi studies on insects. Part II. The optic lobes of Diptera. *Philos Trans R Soc Lond Ser B* 258: 135–223
- Strausfeld NJ (1989) Beneath the compound eye: neuroanatomical analysis and physiological correlates in the study of insect vision. In: Stavenga DG, Hardie RC (eds) *Facets of vision*. Springer, Berlin Heidelberg New York, pp 317–359
- Strausfeld NJ (1998) Crustacean-insect relationships: the use of brain characters to derive phylogeny amongst segmented invertebrates. *Brain Behav Evol* 54: 186–206
- Strausfeld NJ, Bassemir UK (1985) Lobula plate and ocellar interneurons converge onto a cluster of descending neurons leading to neck and leg neuropil in *Calliphora erythrocephala*. *Cell Tissue Res* 240: 617–640
- Strausfeld NJ, Lee J-K (1991) Neuronal basis for parallel visual processing in the fly. *Visual Neurosci* 7: 13–33

- Strausfeld NJ, Kong A, Milde JJ, Gilbert C, Ramaiah L (1995) Oculomotor control in calliphorid flies: GABAergic organization in heterolateral inhibitory pathways *J Comp Neurol* 361: 298–320
- Suga N, Kanwal JS (1995) Echolocation: creating computational maps. In: Arbib MA (ed) *The handbook of brain theory and neural networks*. MIT Press, Cambridge, Mass., pp 344–348
- Theunissen FE, Miller JP (1991) Representation of sensory information in the cricket cercal sensory system. II. Information theoretic calculation of system accuracy and optimal tuning-curve widths of four primary interneurons. *J Neurophysiol* 66: 1690–1703
- Zeil J (1979) A new kind of superposition eye: the compound eye of male Bibionidae. *Nature (Lond)* 278: 249–250